Received: 21 April 2023 | Revised: 23 August 2023 | Accepted: 29 August 2023

DOI: 10.1111/ppl.14021

ORIGINAL RESEARCH

Physiologia Plantarum

A mechanistic mathematical model for describing and predicting the dynamics of high-affinity nitrate intake into roots of maize and other plant species

Laura Zanin[1] | Nicola Tomasi[1] | Daniele Casagrande[2] | Francesco Danuso[1] | Sara Buoso[1] | Anita Zamboni[3] | Zeno Varanini[3] | Roberto Pinton[1] | Franco Blanchini[4]

[1]Department of Agricultural, Food, Environmental and Animal Sciences, University of Udine, Udine, Italy

[2]Dipartimento Politecnico di Ingegneria e Architettura, University of Udine, Udine, Italy

[3]Department of Biotechnology, University of Verona, Verona, Italy

[4]Dipartimento di Matematica, Informatica e Fisica, University of Udine, Udine, Italy

Correspondence
Laura Zanin, Department of Agricultural, Food, Environmental and Animal Sciences, University of Udine, Via delle Scienze 206, 33100 Udine, Italy.
Email: laura.zanin@uniud.it

Funding information
Agritech National Research Center; Departmental Strategic Plan (PSD), University of Udine; European Union Next-Generation EU, Grant/Award Number: Uniud-DM737

Edited by J. Salojärvi

Abstract

A fully mechanistic dynamical model for plant nitrate uptake is presented. Based on physiological and regulatory pathways and based on physical laws, we form a dynamic system mathematically described by seven differential equations. The model evidences the presence of a short-term positive feedback on the high-affinity nitrate uptake, triggered by the presence of nitrate around the roots, which induces its intaking. In the long run, this positive feedback is overridden by two long-term negative feedback loops which drastically reduces the nitrate uptake capacity. These two negative feedbacks are due to the generation of ammonium and amino acids, respectively, and inhibit the synthesis and the activity of high-affinity nitrate transporters. This model faithfully predicts the typical spiking behavior of the nitrate uptake, in which an initial strong increase of nitrate absorption capacity is followed by a drop, which regulates the absorption down to the initial value. The model outcome was compared with experimental data and they fit quite nicely. The model predicts that after the initial exposure of the roots with nitrate, the absorption of the anion strongly increases and that, on the contrary, the intensity of the absorption is limited in presence of ammonium around the roots.

1 | INTRODUCTION

Among plant nutrients, nitrogen (N) is the only one that can be taken up by roots in many different forms, organic and inorganic ones: nitrate, ammonium, urea, oligopeptides, amino acids and others. Under temperate climate conditions, nitrate and ammonium are the two inorganic forms that mainly sustain plant N-needs as they are the most available N-forms in the soil. Plants are able to activate an intricate and complex sensing and signaling network to perceive the availability of different N-forms in the root external solution and, as a consequence, to regulate the acquisition of each N-form (Pinton et al., 2016).

The acquisition of nitrate in plants is a topic that has been deeply investigated and has received great interest among researchers in the last 30 years (Vidal et al., 2020). Among all nutritional pathways, the nitrate pathway (from its transport to signaling network) is one of the most studied. It is known that nitrate can be taken up by roots through different transport systems, the so-called Low-Affinity Transport System (LATS) and High-Affinity Transport System (HATS; Daniel-Vedel et al., 1998). Under aerobic soil conditions, the nitrate

concentration in soil solution is estimated to range from 0.1 to 1 mM. Below 1 mM nitrate, the acquisition of this N-form is mainly mediated by HATS. Some transporters are constitutively expressed in plants, whereas others display inducible features depending on the availability of nitrate and other N-forms in the root external solution (Hole et al., 1990). Under N-starvation, the gene expression of NRT2 transporters (in Arabidopsis AtNRT2.1 and AtNRT2.2, main components of inducible HATS, iHATS) is induced by nitrate taken up by a constitutive double affinity transporter (AtNRT1.1, main component of constitutive HATS, cHATS; Krouk et al., 2006; Wang et al., 1998). Several other proteins (including transporters, enzymes, transcription factors, and accessory proteins) are involved in the acquisition of nitrate (for review, see Krouk et al., 2010a; Vidal et al., 2020). A key role in the nitrate induction process is played by NAR2/NRT3, an accessory protein required for the full functionality of iHATS (Kotur et al., 2012; Li et al., 2007; Orsel et al., 2006). At transcriptional level, the upregulation of NAR2/NRT3 gene appears to be strongly responsive to the availability of nitrate in the root external media, and its maximum level of expression comes before the maximum upregulation of inducible NRT2s' transporters (Pii et al., 2014; Zanin et al., 2015). In addition to its effect on transport activity, NAR2.1 also appears to be involved in NRT2.1 stabilization and localization at the plasma membrane (Wirth et al., 2007).

The phenomenon of nitrate-transport induction has been proven to occur also in soil (Varanini et al., 2018), as roots are exposed to frequent fluctuations in nitrate availability in the soil solution. This implies that roots need to promptly adapt the activity of their nitrate uptake systems to acquire this nutrient efficiently. Considering the need for sustainable agriculture, the relationship between the nitrate induction process and the efficiency of N acquisition in plants is an important aspect to evaluate for fertilization management (Liu et al., 2015; Zamboni et al., 2014). In this context, Glass (2003) provided indications that the high-affinity transport system works at high capacity only when plants are N-starved. This implies that breeding programs should select new varieties under nutrient-limiting conditions to identify crops that are able to use N more efficiently. Depending also on the genotypes, plants exhibit great variability in the phenomenon of nitrate induction. Two inbred lines of maize with different NUE (Lo5 and T250; Balconi et al., 1997) have been shown to display different induction times when exposed to the same concentration of the anion (Locci et al., 2001; Varanini et al., 2018; Zamboni et al., 2014). Interestingly, the maize line with the highest NUE (Lo5) induced the maximum uptake rate of nitrate 4 h after the supply with 0.2 mmol L^{-1} nitrate, whereas T250 displayed a late response (the peak of nitrate acquisition was reached after 12 h of exposure to the anion). These studies might indicate that promptness of the induction response is an important trait of high-NUE crops (Garnett et al., 2015).

One famous scheme of action for nitrate acquisition was first outlined by Glass et al. (2002), who clearly described the occurrence of a positive feedback and some negative feedbacks on the regulation of nitrate acquisition. After 20 years of research, experimental evidence indicates this process is tightly regulated at multiple levels: transcriptional, post-transcriptional, and post-translational levels. When nitrate is available in the root external solution, the constitutive expression of NRT1.1 allows a basal intake of nitrate that activates positive feedback at the transcriptional level to activate the expression of NRT2 genes. The assimilation of nitrate into amino acids leads to an increase of ammonium and glutamine concentration in the root cells, two metabolites that cause strong negative feedback on nitrate uptake (Lejay et al., 1999; Nazoa et al., 2003; Zhuo et al., 1999). Moreover, at high external nitrate concentration, a self-inhibition mechanism mediated by NRT1.1 has also been described to regulate the HATS activity at the transcriptionally level (Krouk et al., 2006; Muños et al., 2004).

The dynamic of nitrate acquisition has been described in several plant species (in Arabidopsis, maize and other plant species; Araki and Hasegawa, 2006; Aslam et al., 1993; Behl et al., 1988; Cesco et al., 2002; Kronzucker et al., 1995; Massaro et al., 2019; Min et al., 1998; Monte et al., 2006; Zamboni et al., 2014; Pii et al., 2014; Tomasi et al., 2015; Zanin et al., 2015, 2018, 2022). The occurrence of positive and negative feedbacks shapes the pattern of net-nitrate influx in roots. Commonly, after a few hours of root exposure to nitrate, a peak of maximum nitrate intake rate is reached and (in the following hours) a retro-regulation of the system limits the nitrate uptake rate. This tight regulation of nitrate uptake rate is operated mainly by N assimilates (as ammonium and glutamine) to match the net influx of nitrate in roots with the plant capacity of N organization. In this way, root cells prevent the waste of energy and reductive power in root cells as well as the production of harmful intermediates (as nitrite, nitric oxide, and ammonium/ammonia). Thus, plants are able to activate a prompt control of nitrate uptake, a spatiotemporal regulation that plays a key role in guaranteeing plant resilience upon environmental stresses (Boer et al., 2020).

From a mathematical point of view, the modeling of nitrate uptake in plants helps the description of this process and may provide new information on the mechanistic regulation of the entire system, including the development of root system architecture in response to diverse N-forms (Araya et al., 2016).

A previous important study (Cacco et al., 2002) investigated the induction and feedback inhibition of nitrate uptake using three time-dependent differential equations. Our model allows for a step beyond as we model the overall absorption mechanism starting from its essential building blocks. In particular, the model by Cacco et al. (2002, eq. (3)) introduced a time-dependent rule, which is an a priori-decided increasing function of time, they call the induced time-dependent uptake rate, to reproduce the data. In our analysis, we do not need to introduce any time-dependent prepackaged function, and the increasing–decreasing behavior is an outcome of the model.

Other approaches (Le Deunff and Malagoli, 2014; Le Deunff et al., 2019; Malagoli and Le Deunff, 2014; Malagoli et al., 2004) have integrated the information on nitrate acquisition, biomass production, root development, and environmental conditions to provide an important predictive tool to assist precision farming management during the whole growth cycle. A based flow–force approach (applied to nitrate influx isotherms and experimentally determined environmental and in

planta regulation) was used to model nitrate uptake in oilseed rape, *Brassica napus* (Le Deunff and Malagoli, 2014; Le Deunff et al., 2019; Malagoli and Le Deunff, 2014). However, our dynamic model is different in nature, being concerned mainly with the evolution in time of absorption. In Cardenas-Navarro et al. (1999), the authors proposed a model based on "phases," qualitatively described without resorting to differential equations as we do to obtain a prediction of the absorption time evolution. Differential equations are successfully adopted in Boer et al. (2020), yet the focus of that work is on the relation of absorption with root growth. Their model is tuned on a completely different time scale (the absorption analyzed on a period of 6–8 days) and a strictly increasing function of time is detected.

In our model, we explain the mechanistic process of nitrate uptake, on a time horizon of several hours, using seven differential equations. The complexity of our model allowed us to parameterize precisely the single components involved in the nitrate acquisition and, therefore, allowed an accurate estimation of the plant response when even ammonium was added with nitrate in the external solution. The model is mechanistic as it is based on the modeling of the relevant reactions based on physical laws expressed in terms of linear terms as well as Hill functions. The model evidences the presence of a short-term positive loop, acting in the first few hours, which has the effect of boosting the nitrate intake by promoting the synthesis of functional proteins. Two additional negative loops by nitrate reduction products (ammonium and amino acids) are also considered and cause (in the long run, ca. 6–12 h) the inhibition of the nitrate intake proteins, "shutting down" the absorption. Additionally, the model evaluates the dynamic of the nitrate concentration in the vacuole as well as the reservoir of nitrate transporters in vesicles for their targeting to the plasma membrane. We do not impose any prepackaged behavior: the initial rapid growth and the final inhibition is an outcome of the modeled mechanism.

The model fits well with experimental data obtained from different plant species and it predicts quite accurately the effect of the presence of ammonium, which can reduce, or even eliminate, the peak of net-uptake rate of nitrate. The validation of the model confirms that it may be a fruitful tool to correctly predict the pattern of net-nitrate acquisition in plants according to genetic variation and nutrient availability in the root external solution.

2 | MATERIALS AND METHODS

2.1 | Plant material and growth conditions

Maize plants (*Zea mays* L., P0423, Pioneer Hybrid Italia S.p.A.) and wheat (*Triticum aestivum*, var. Palladio) were hydroponically grown as previously described in Zanin et al. (2015). Therefore, after germination over aerated 0.5 mM $CaSO_4$ solution, seedlings (3-day old) were transferred into an aerated hydroponic system under controlled conditions (16/8 h light/dark cycle, 220 μmol m^{-2} s^{-1} light intensity, 25/20°C temperature, 70–80% relative humidity). After 2 days, all plants (5-day old) were transferred to a N-free nutrient solution (μM: $CaSO_4$ 500; KH_2PO_4 175; $MgSO_4$ 100; NaFe-EDTA 20; KCl 5; H_3BO_3 2.5; $MnSO_4$ 0.2; $ZnSO_4$ 0.2; $CuSO_4$ 0.05; Na_2MoO_4 0.05). As control, a batch of plants was kept under this N-free condition (*−N* treatment), whereas in the pots of the other plants N was added in the form of nitrate or nitrate plus ammonium: 0.5 mM $Ca(NO_3)_2$ was added to *Nitrate* treated plants, 0.5 mM $Ca(NO_3)_2$ plus 0.05 mM $(NH_4)_2SO_4$ were added to *Nitrate + 0.1* mM *Ammonium* treated plants, 0.5 mM $Ca(NO_3)_2$ plus 0.25 mM $(NH_4)_2SO_4$ were added to *Nitrate + 0.5* mM *Ammonium* treated plants, 0.5 mM $Ca(NO_3)_2$ plus 0.5 mM $(NH_4)_2SO_4$ were added to *Nitrate + 1.0* mM *Ammonium* treated plants. Therefore, five treatments were performed: *−N*, *Nitrate*, *Nitrate + 0.1* mM *Ammonium*, *Nitrate + 0.5* mM *Ammonium*, *Nitrate + 1.0* mM *Ammonium* treatments. Nitrogen-forms were added to N-free nutrient solution an hour after the beginning of the light phase (time: 0 h of treatment). Using potassium hydroxide (KOH), the solution pH was adjusted to 6.0.

2.2 | Measurements of net high-affinity nitrate uptake

After 0, 2, 4, 6, 8, 10 and 24 h of treatment and for each nutritional treatment, the roots of six intact plants were sampled, and grouped in pairs (each consisting of two plants, three biological replicates $N = 3$) for the evaluation of the net influx of nitrate by depletion from a solution containing 200 μM KNO_3 for 10 min as described by Pinton et al. (1999). Changes in nitrate concentration were determined spectrophotometrically at 410 nm as described by Cataldo et al. (1975).

2.3 | Data analyses

In order to give an explanation of the measured data, the main processes involving nitrate have been considered and written as dynamic equations describing (in the form of an algebraic sum of fluxes) the rate of variation of the main quantity concentrations. Each equation is characterized by parameters, every choice of which gives rise to a specific model instance. One of the consequences of considering a parametric structure is that the nitrate concentration predicted by the model, which is the output of the dynamic system, depends on the values of the parameters. The calibration consists in the search for the values of the parameters that give the best fitting to the collected measurements, namely which values best match the experimental data with the output predicted by the model.

3 | RESULTS

3.1 | Experimental data collection: Measure of net nitrate uptake rate in plants

The experimental setup used 5-day-old maize seedlings that were exposed or not to nitrate (1 mM nitrate) and, at each sampling time,

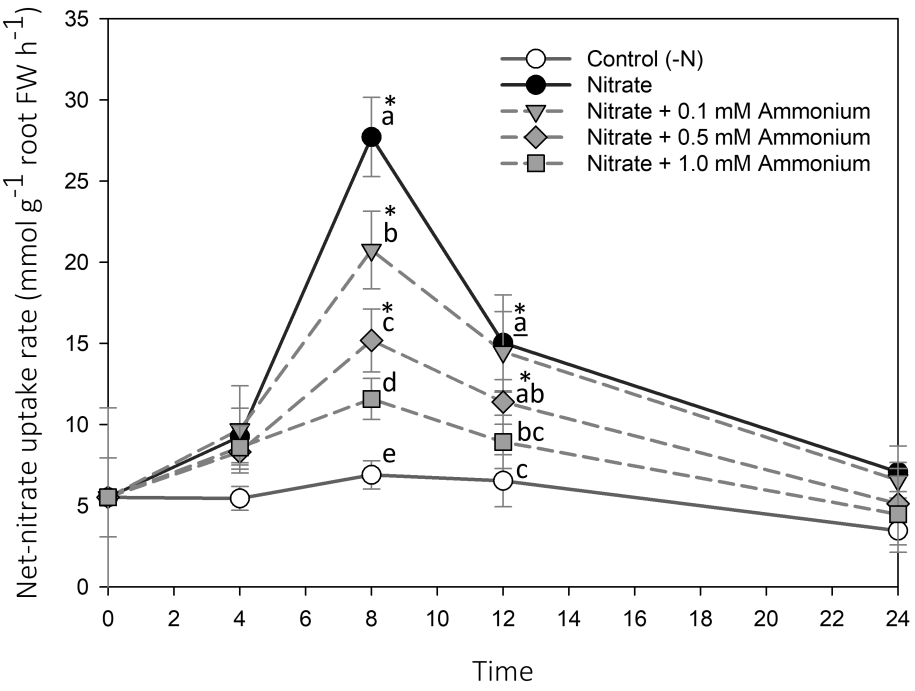

FIGURE 1 Nitrate net-uptake in roots of maize. Five-day-old maize seedlings were exposed for a maximum of 24 h to N-free nutrient solution (*−N* treatment) or to nutrient solution containing N in form of nitrate (1.0 mM) and ammonium (0.0, 0.1, 0.5, or 1.0 mM ammonium, respectively: *Nitrate* treatment, *Nitrate + 0.1* mM *Ammonium treatment*, *Nitrate + 0.5* mM *Ammonium* treatment, *Nitrate + 1.0* mM *Ammonium* treatment). Net nitrate uptake was measured by depletion from a solution containing 0.2 mM nitrate (letters refer to statistical significance within each thesis, asterisks refer to statistical significance between each timepoint and the starting point (−vs. $t = 0$ h), one-way ANOVA, Holm Siddak test, $N = 3$, $p < 0.05$)

the roots of intact plants were transferred to an assay solution containing 0.2 mM nitrate. By depletion method, we evaluated the disappearance of nitrate from the root external solution. During the time span of 10 min, the reduction of nitrate concentration in the root external solution provided an indirect measure of net-nitrate influx into roots.

Plant exposure to nitrate (*Nitrate* plants) determined a transient induction of its uptake rate reaching a maximum value (after 8 h in hybrid maize P0423) due to the activation of a "feedback inhibition." On the other hand, untreated plants (plants not exposed to nitrate, *−N* plants) did not significantly change the uptake rate of nitrate during the time span of 24 h.

When ammonium was added to the nitrate-containing nutrient solution, the pattern of nitrate acquisition showed a reduction in the maximum uptake rate. The presence of 0.1, 0.5 or 1.0 mM ammonium reduced the entity of nitrate net-influx by 25, 45 and 58%, respectively, at 8 h in comparison to the maximum uptake rate reached by *Nitrate* plants (Figure 1).

3.2 | Mathematical modeling of nitrate uptake rate

We propose a dynamical mechanistic model aiming at explaining the uptake process in physical terms. The model is compartmental-like and governed by seven differential equations. The corresponding seven state variables represent concentrations of elements in proper compartments (see Table 1).

Most of the interactions are indeed related to transport or assimilatory process of nitrate and can be associated with flows from one state variable to another. In Figure 2, these flows are represented by blue arrows. These flows are assumed proportional to the concentrations in the compartments they originate.

TABLE 1 The parameters considered in the model are provided in the table

Description	Symbol	Associated variable
Nitrate concentration	NO_3^-	x_1
Nitrite concentration	NO_2^-	x_2
Ammonium concentration	NH_4^+	x_3
Amino acids' concentration	aa	x_4
Nitrate transporters (intaking activating proteins)	TS	x_5
Nitrate transporters in the molecular vesicles	TS_{res}	x_6
Nitrate stored in the vacuole	NO_3^- res	x_7

Abbreviations: aa, amino acids; res, reserve, TS, transporters.

The corresponding differential equations are

$$\dot{x_1} = \underbrace{u_0 + \theta f_5(x_5) - \xi x_1}_{\text{flow intake}} - \alpha x_1 - \omega x_1 - \mu x_1 + \nu x_7,$$

$$\dot{x_2} = \alpha x_1 - \beta x_2,$$

$$\dot{x_3} = \beta x_2 - \gamma x_3,$$

$$\dot{x_4} = \gamma x_3 - \delta x_4,$$

$$\dot{x_5} = u_1 x_1 [\epsilon g_3(x_3) + \phi g_4(x_4)] - \eta x_5 - \rho x_5 + \sigma x_6,$$

$$\dot{x_6} = \rho x_5 - \sigma x_6,$$

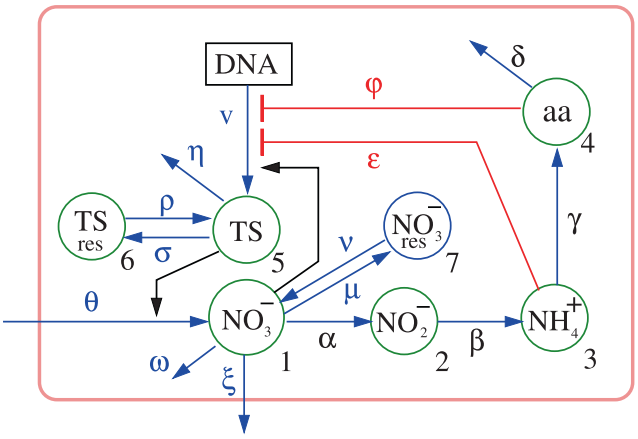

FIGURE 2 Representative model of nitrate acquisition in roots. Positive and negative feedbacks operating on HATS are indicated: blue arcs represent flows, black and red arcs represent positive and negative feedback regulation, respectively. TS_{res}, reservoir of nitrate transporters in vesicles; $NO_3^-{}_{res}$, reservoir of nitrate in the vacuole; *aa*, amino acids

$$\dot{x_7} = \mu x_1 - \nu x_7.$$

The proportionality constants (model parameters) are denoted by Greek letters as follows:

- α, quantifies the reduction of nitrate to nitrite;
- β, quantifies the reduction of nitrite to ammonium;
- γ, quantifies the reactions of assimilation of ammonium into amino acids;
- δ, accounts for the subsequent reactions of transamination, protein synthesis and transport processes to other parts of the plant;
- μ,ν, quantify the (nitrate) flows into the vacuole and out from it, respectively;
- η, quantifies the natural protein degradation, including the components involved in the nitrate acquisition process;
- ρ, σ, quantify the flows of proteins into the vesicles and out of them, respectively;
- ξ, quantifies the (nitrate) outflow from the cells (affected by the NAXT carrier);
- ω, accounts for the translocation of nitrate;
- θ, is the coefficient of the protein induced intake.

The model considers the processes of gene transcriptional flow:

$$u_1 x_1 [\epsilon g_3(x_3) + \phi g_4(x_4)],$$

in which the factor $u_1 x_1$ represents the activation due to the nitrate x_1 (represented by a black arrow in Figure 2), while the term in square brackets includes two decreasing threshold-type functions of the ammonium (x_3) and of the amino acids (x_4) that act as inhibitors (red arcs). Such inhibiting effects are modeled by decreasing Hill functions, denoted by g_3 and g_4, respectively and defined by

$$g_3(x_3) = \frac{1}{1 + (x_3/\overline{x_3})^q} \qquad g_4(x_4) = \frac{1}{1 + (x_4/\overline{x_4})^q}$$

where q is a positive number while $\overline{x_3}$ and $\overline{x_4}$ are threshold values for the ammonium and the amino acids, respectively. For small values of variables x_3 and x_4, the value of the functions g_3 and g_4 is approximately one, hence the corresponding gene transcriptional flow is $u_1 x_1 [\epsilon + \phi]$. Conversely, as x_3 and x_4 increase, both g_3 and g_4 tend to zero, hence the flow drops to 0 for large values of x_3 and x_4. The term u_1 is an input of the system representing the intrinsic capability of synthesized nitrate transporters. Coefficient q represents the sharpness of the inhibition: for large, ideally infinite q, the inhibition is switched on immediately after the threshold.

The nitrate entering flow is the sum of a constant term u_0 representing a natural incoming flow and a term $\theta f_5(x_5)$, which is variable, according to the plant capability of adsorbing nitrate. This capability, in turn, is described by an increasing threshold-like Hill function f_5,

$$f_5(x_5) = \frac{(x_5/\overline{x_5})^p}{1 + (x_5/\overline{x_5})^p},$$

where, again, $\overline{x_5}$ is a threshold value beyond which the activating effect of x_5 begins.

The flow intake term present in the first equation is associated with $\dot{x_1}$ and it is

$$u_0 + \theta f_5(x_5) - \xi x_1.$$

We see that three terms appear in the above expression: u_0, which is the naturally induced inflow; $\theta f_5(x_5)$, which has been previously described and represents the protein-induced intake, and $-\xi x_1$, which is the outflow due to natural permeability. We also assume the following:

1. The natural flow u_0 is assumed to be given by the following expression:

$$u_0 = \text{conc}_{\text{nit}} f_{\text{bas}},$$

namely, it is the product of the external nitrate concentration and a coefficient f_{bas} characteristic of the plant.

2. The protein-induced component $\theta f_5(x_5)$ is assumed independent of the external nitrate concentration. It depends only on the quantity of protein x_5, which is activated by the positive feedback and governed by the threshold function $f_5(x_5)$.

The system output is the overall nitrate-absorbing capability measured in our experiments. We assume that this quantity is given by the next expression,

$$y = \mathrm{conc}_{\mathrm{meas}} f_{\mathrm{bas}} + \theta f_5(x_5) - \xi x_1.$$

The rationale for this choice is that, under experimental conditions, the quantity of nitrate is standard and fixed once and for all. Note that the former term $\mathrm{conc}_{\mathrm{nit}} f_{\mathrm{bas}}$ has now been replaced by $\mathrm{conc}_{\mathrm{meas}} f_{\mathrm{bas}}$ just to make it clear that, under experimental conditions, the nitrate concentration $\mathrm{conc}_{\mathrm{meas}}$ is standard and fixed. In our experiments we assume $\mathrm{conc}_{\mathrm{meas}} = 0.2$.

The term $\theta f_5(x_5)$, accounting for the positive-feedback induced inflow, is not directly influenced by the experimental nitrate concentration. Yet it represents a large portion of the absorption. In the transient this term is initially zero, in practice very small, unless the plant has been previously exposed to nitrate. Indeed a preliminary exposure to nitrate activates the positive feedback chain $x_1 \to x_5$, from the beginning of the experiment, making the absorption peak higher and immediate.

3.3 | Model fitting to data

To evaluate the validity of the model described above, experimental measurements concerning the nitrate concentration in different situations and for different plants have been collected. These data, which should be reproduced by the output of the model, have then been fitted by properly choosing the values of the parameters appearing in the equations. The optimal choice of these values has been performed by a *trial-and-error* strategy. In particular, the experiments have been made considering different plants (for the same concentration) as well as different concentrations (for the same plant) and they are summarized in Table S1, Supporting Information where each experiment is associated with a letter and with the number of the figure in which results are reported. Values of the parameters that fit the data well are reported in Tables S2 and S3.

As a first remark, it can be noted that, for each set of measurements, there exists (at least) a set of parameter values, precisely the ones reported in Tables S2 and S3, which fit quite well the experimental data. However, as one may expect, since the number of parameters is redundant with respect to the measured quantities, the values listed in the tables are not the only possible choice to fit the data. In fact, among all trials performed, different choices associated with similar data fitting, not reported for brevity, have been evaluated. Obviously, this variability of values could be reduced if measurements associated with quantities other than the nitrite concentration were available and this fact could lead to future developments of the investigation.

Another interesting result, which is evident from Tables S2 and S3, is that, especially for plants belonging to the same species, many parameters have the same values regardless the experiment, while only a few characterize the response of the system to different operating conditions. Compare, for instance, the entries of the columns E, F, G, H and I, associated with the response of the *Z. mays* Lo5, where to fit data corresponding to different nitrate concentrations, it is sufficient to vary the values of two parameters.

Finally, it is worth observing that, to simplify the fitting procedure, in some cases, it could be convenient to re-scale the horizontal axis of the output of the dynamical system, that is, the time, or the vertical axis, that is, its magnitude (or both). This action has been performed in some of the fitting procedures; they are displayed by "Time scale" and "Magnitude factor" values as indicated in Table S3.

3.4 | Model implementation in SEMoLa

The nitrate uptake model has been implemented in SEMoLa language (Danuso and Rocca, 2014) with the name of *NitrUp* (Figure S1).

SEMoLa (Simple, Easy to use, Modeling Language) is a declarative language with a software framework for the development of simulation models. It allows the representation of dynamic systems with the capability of dealing with deterministic or stochastic models based on states (tanks and flows), on elements (such as individual-based models) and on discrete events. The ontology of the SEMoLa language derives from the System Dynamics approach proposed by Forrester (1968). The code of SEMoLa models is easily understandable and modifiable even by non-programmers. *NitrUp* can be launched (under Windows OS) by itself from the console window, from other software as a command line or using the *SemRun* application (a runner for SEMoLa models), included in the *NitrUp* installation package.

NitrUp allows carrying out simulation experiments, sensitivity analysis of parameters and their automatic calibration, statistical processing of measured and simulated data, graphical display of observed/simulated variables and automating procedures using scripts.

The installation package also includes the source code of the model (in SEMoLa language), which can be modified within the SEMoLa framework to create new versions of the model.

4 | DISCUSSION

The substrate-inducible feature of the nitrate high-affinity transport system in roots has been characterized in many plant species (Jackson et al., 1973; Orsel et al., 2002; Pinton et al., 2016; Santi et al., 2003). In the present work, we provide a mathematical description of the model of net-nitrate acquisition in maize, and we demonstrate its validity for other plant species (wheat, grapevine, arabidopsis). Considering the whole process, the dynamic of the nitrate influx can be studied using a multidisciplinary approach, and mathematical modeling may allow deciphering the regulation of this mechanism, hence predicting the nitrate acquisition response of plants. Indeed, benefiting from new results and data collected over the years, a data fitting elaboration was performed using Arabidopsis, wheat, and grapevine experimental data to find the best value of each parameter to adapt the model to different plant species.

The proposed mechanistic model was designed starting from biological processes involved in nitrate transport, assimilation and their regulation (Figure 2). Our building blocks are biochemical laws

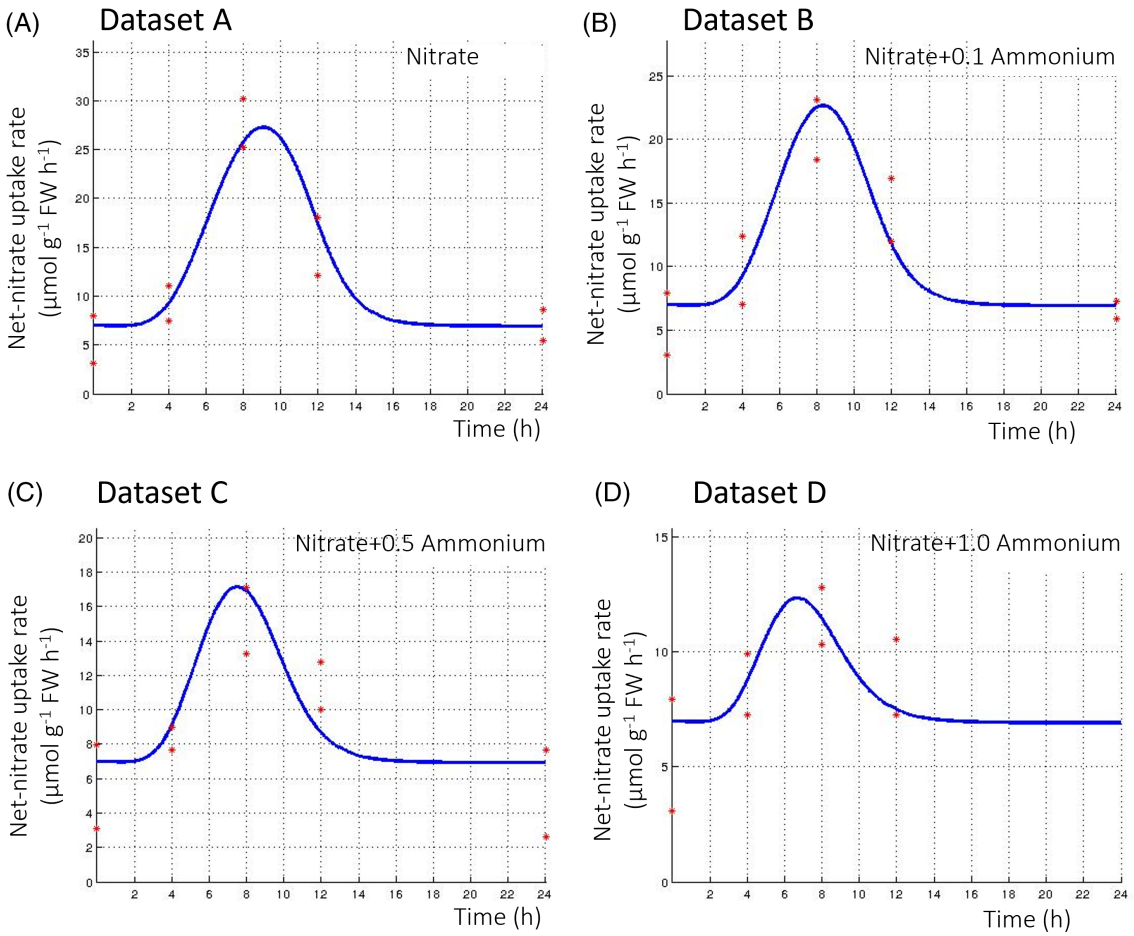

FIGURE 3 Comparison of the model simulation (blue lines) with the experimental data of (A) *Nitrate* treatment maize plants (dataset A), (B) *Nitrate* + *0.1 Ammonium* treatment plants (dataset B), (C) *Nitrate* + *0.5 Ammonium* treatment plants (dataset C), (D) *Nitrate* + *1.0 Ammonium* treatment plants (dataset D). Red asterisks refer to the range, above and below, of ±standard deviation from the average values collected by experimental analyses (Figure 1). The alphabetic numerals of the datasets refer to Table S1

expressed in terms of Hill function, compartmental flows suitably combined to derive a system of differential equations. The resulting dynamical model has been adopted to describe nitrate acquisition process over time. The outputs of this mechanistic model have been compared with experimental data to test its validity (Figure 3). The output of the model was an induction and deinduction curve of net-nitrate-uptake rate over time, having a pattern reproducing quite faithfully the one obtained from experimental data. The values of the equations' parameters have been optimized to fit the model outputs to the experimental data on maize. Nevertheless, our mechanistic model has proven to be easily adaptable to describe the response of other plant species as it requires only a new specific adaptation of the parametric values (Figures 4–6 and Tables S1–S3).

Our experimental data (Figure 1) confirms the famous scheme for the nitrate induction regulatory process first reported by Glass et al. (2002), who showed that the nitrate acquisition is a process feedback-regulated: it is induced by the presence of nitrate and negatively regulated by nitrate assimilatory products (such as ammonium and glutamine). During the last decades, different levels of regulation have been characterized (Ho et al., 2009; Krouk et al., 2010b). In the light of these findings, we propose a new and more detailed mechanistic model that evidences multiple levels of regulation of nitrate net-influx: a transcriptional- and a post-translational regulation on nitrate transporters, nitrate translocation to other plant organs, nitrate efflux from the root cells, nitrate assimilation, nitrate vacuolar storage, amino acids' translocation, usage and negative feedback by assimilatory products at transcriptional level on nitrate transport system (Figure 2). Moreover, we propose a regulation on the nitrate transport system activity via bi-directional trafficking between an internal pool of vesicles, containing the transporters, similarly to what has been described for iron and proposed for urea transporters (Barberon et al., 2014; Pinton et al., 2016; Tan et al., 2022).

Based on these considerations, we transcribe our mechanistic model (Figure 2) in mathematical terms to predict the dynamic of the nitrate influx into plants in function of the nitrate available to the roots. With respect to the existing models, which are not mechanistic but rather best-fitting equation that describes retrospectively experimental data (Cacco et al., 2002; Devienne-Barret et al., 2000; Le Deunff et al., 2019), our model provides a more detailed insight, and is suitable for predictions including, quite notably, the effect of the

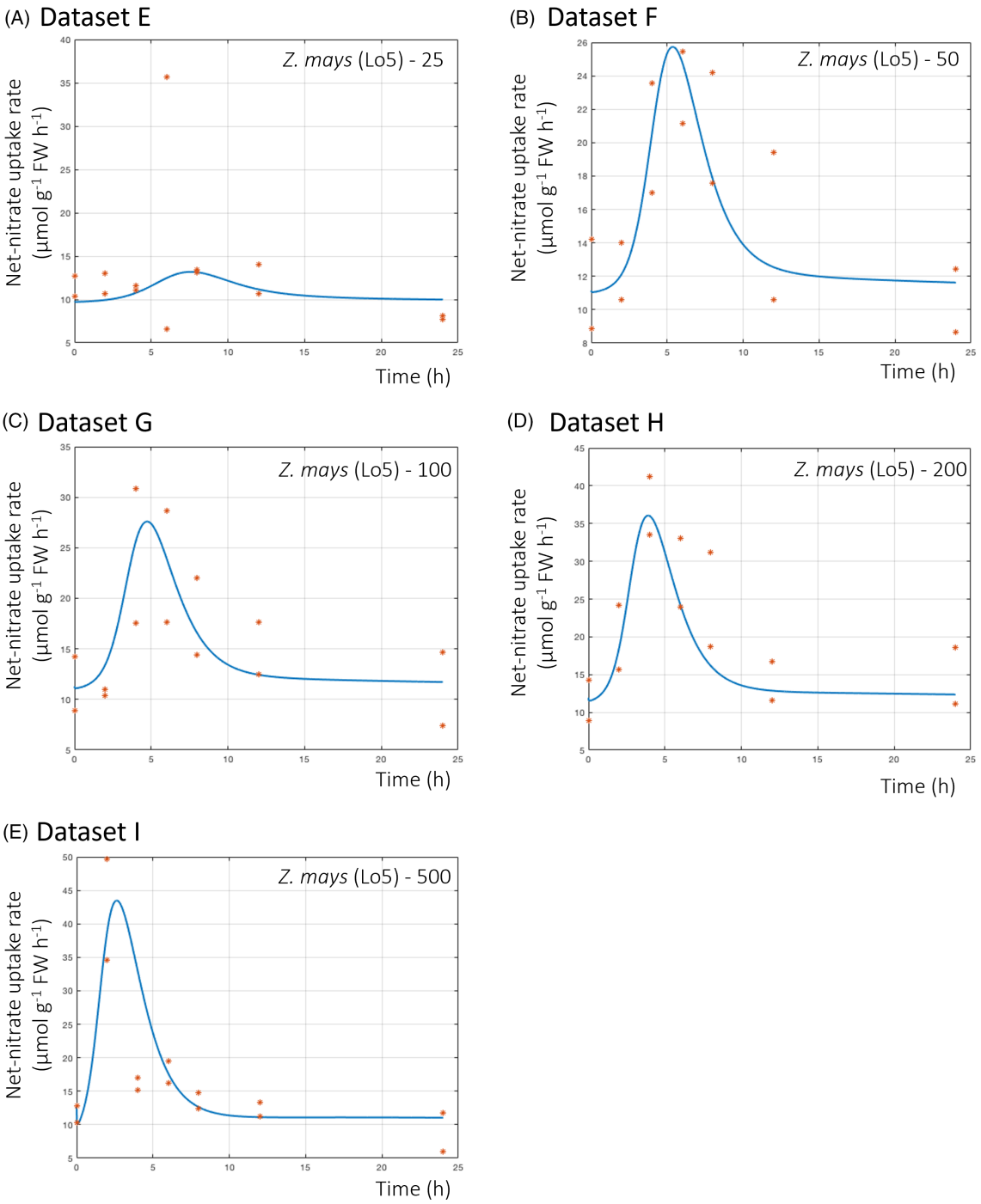

FIGURE 4 Comparison of the model simulation (blue lines) with the experimental data measured in *Z. mays* Lo5 after exposure to different nitrate concentrations: (A) 0.025 mM nitrate (dataset E), (B) 0.050 mM nitrate (dataset F), (C) 0.100 mM nitrate (dataset G), (D) 0.200 mM nitrate (dataset H), (E) 0.500 mM nitrate (dataset I). Red asterisks refer to the range, above and below, of ±standard deviation from the average values collected by experimental analyses (Zamboni et al., 2014). The alphabetic numerals of the datasets refer to Table S1

presence of ammonium at the beginning of the process. Inspired by the work of Cacco et al. (2002), we intended to explain the absorption process that is initially rapidly increasing and eventually decreasing. Cacco et al. (2002) have proposed a model based on the product of two functions of time, one increasing and one asymptotically decreasing and converging to zero, which reproduce faithfully the data.

In our mechanistic model, we confirm their findings by explaining that this increasing–decreasing absorption is due to two specific regulation mechanisms acting at different times. Precisely, we show that the positive regulation is associated with an initial absorption increase, followed by a negative regulation that causes a decrease of the absorption. More precisely, our mechanistic model summarizes

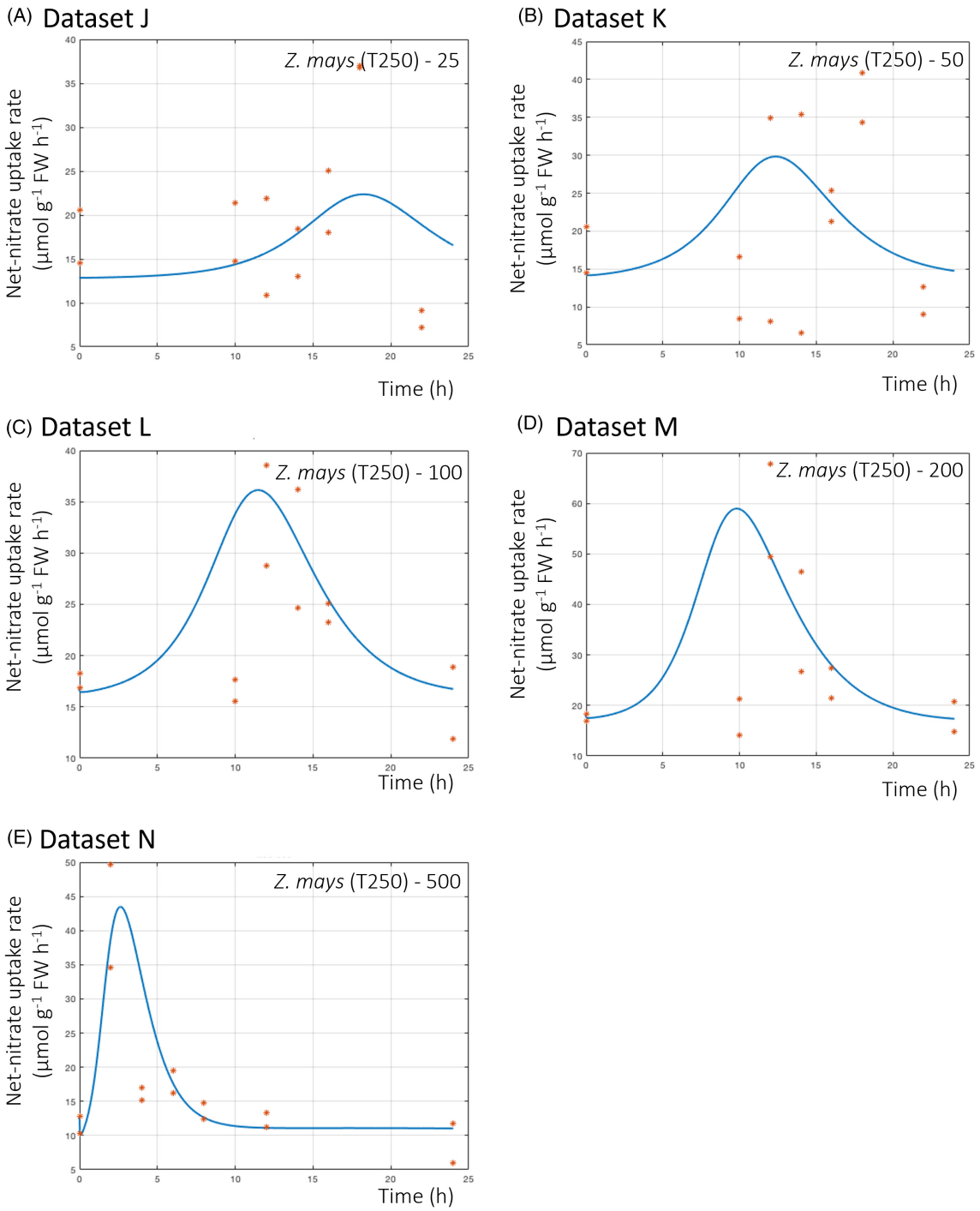

FIGURE 5 Comparison of the model simulation (blue lines) with the experimental data measured in *Z. mays* T250 after exposure to different nitrate concentrations: (A) 0.025 mM nitrate (dataset J), (B) 0.050 mM nitrate (dataset K), (C) 0.100 mM nitrate (dataset L), (D) 0.200 mM nitrate (dataset M), (E) 0.500 mM nitrate (dataset N). Red asterisks refer to the range, above and below, of ±standard deviation from the average values collected by experimental analyses (Zamboni et al., 2014). The alphabetic numerals of the datasets refer to Table S1

the effects of the occurrence of positive and negative regulations. In our model, the basal effect (i.e., excluding the loops), in which we have u_0 depending on the external nitrate availability, is not subject to feedback regulation. At low nitrate concentrations (in the micromolar range), the u_0 component, along with the efflux component of nitrate (represented by the function $-\xi x_1$), defines the basal or constitutive acquisition of nitrate in root cells. The efflux component $-\xi x_1$ is mediated by a unidirectional transporter, named NAXT1 in Arabidopsis, that is responsible for the passive nitrate efflux at the root plasma membrane. Physiological evidence confirmed that, in contrast to the influx, the nitrate efflux is a thermodynamically downhill process (Miller et al., 2007; Segonzac et al., 2007). Thus, the presence of this

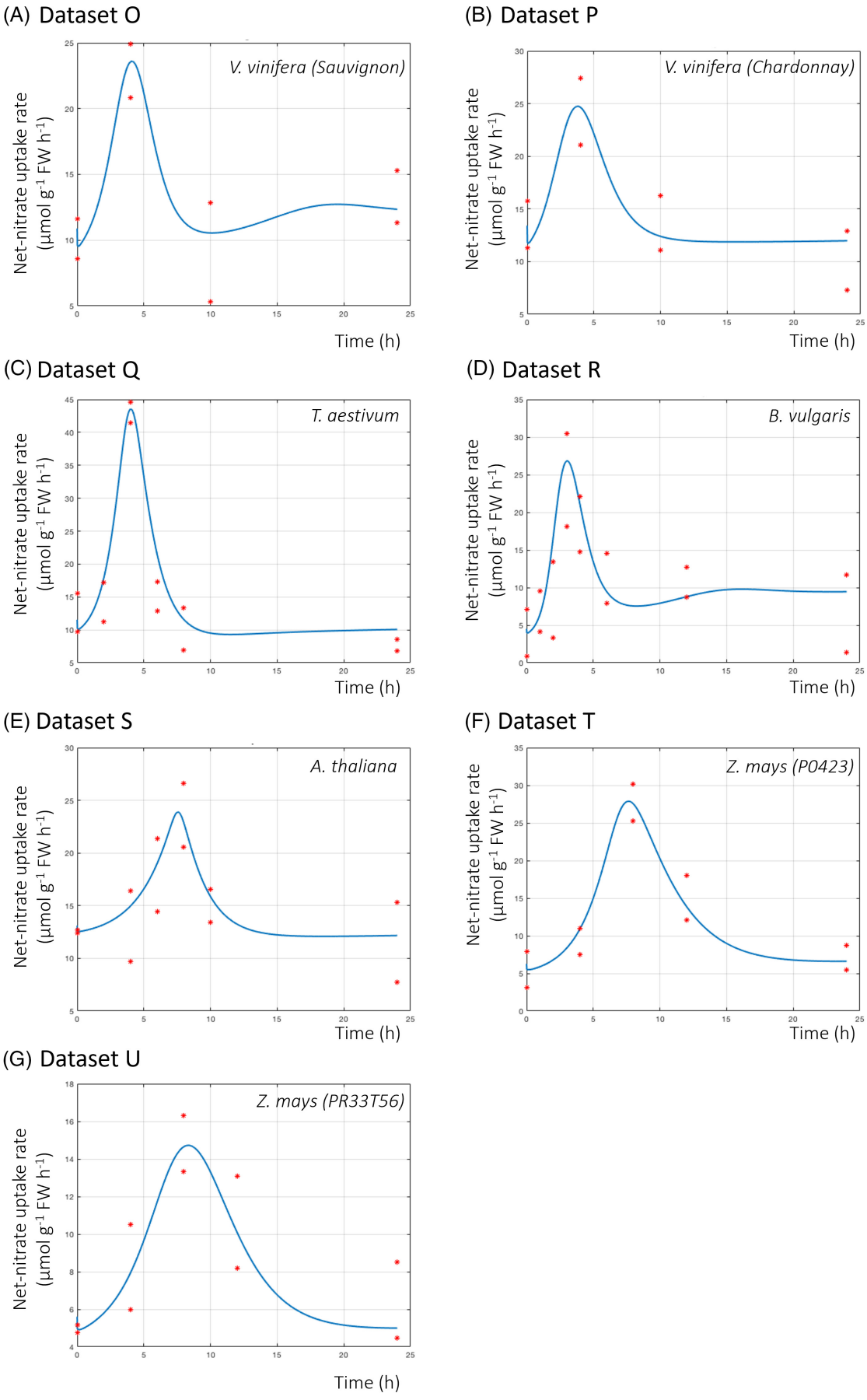

FIGURE 6 Legend on next page.

component prevents the system from becoming overloaded with nitrate when root cells are unable to assimilate, store or translocate the anion.

On the top of this basal acquisition process, we distinguish three loops sequentially activated with different timing: (1) a positive loop is activated in the short term, which increases nitrate intake. Such a positive loop involves the uptake of nitrate into root cells through two transport systems (cHATS and iHATS) that exhibit a constitutive and an inducible response at the physiological level; (2) a negative loop, acts in the middle term and is based to the inhibitory effect of the nitrate on the transporter production; (3) a long-term negative loop characterized by a dual action that fine-tunes nutrient acquisition to prevent the effects of nitrate overloading on plants, which in turn may lead to oxidative stress and phytotoxic damage in plant cells (such as fast consumption of reducing equivalents, overproduction of nitric oxide and ammonia).

At the experimental level, the basal nitrate flow intake can be estimated by measuring the potential net-nitrate acquisition in N-deficient plants. To measure the potential influx rate, plants are exposed to nitrate only during the time of analysis (10 min). Since these plants were not exposed to nitrate before the analysis, they did not express, at the transcriptional or post-translational level, the machinery needed for an over-acquisition of nitrate. The basal acquisition of nitrate by HATS in N-deficient plants depends on nitrate concentration in the nutrient solution, on the species-dependent basal amount of nitrate acquisition (as shown by not-induced plants: *control (−N)* in Figure 1) and on phenological stage. This pattern is related to the constitutive transport system of nitrate (cHATS), which involves a transporter (NRT1.1) with constitutive gene expression to ensure potential nitrate intake by plants as soon as the anion becomes available in the external root solution. Besides its function as transporter, NRT1.1 works also as a nitrate sensor for the presence of nitrate in the surrounding root solution (that is why its name "transceptor"; Ho et al., 2009; Maghiaoui et al., 2020). When higher concentration of nitrate becomes available in the rhizosphere, the increased basal intake of nitrate (mediated by cHATS) activates the plant response that accounts for the induction of genes encoding iHATS transporters in root cells (Zanin et al., 2015). At physiological level, this response leads to an increase in the high-affinity uptake rate of nitrate, thus nitrate itself acts as a positive effector of its intake.

To model these mechanisms, we have taken into account the kinetic properties of the nitrate acquisition system, especially of iHATS. The activities of nitrate high-affinity transport and assimilation display kinetics that fit with the Michaelis–Menten equation (Devienne-Barret et al., 2000; Ishiyama et al., 2004; King et al., 1992; Le Denuff et al., 2019; Nakano et al., 2012). Thus, in the formula, we used Hill-type functions with $p > 1$ that are known to fit well with a joint effect of Michaelis–Menten enzymes.

In our model, the "negative regulation" or "feedback inhibition" (Siddiqi et al., 1989) was modeled without referring to one specific molecular mechanism but rather evaluating the overall complex regulation operated mainly by metabolic products, a process that implies the involvement of several N-metabolites, a gene regulatory network, cellular compartments and plant organs (King et al., 1993). Unlike positive feedback, which is mediated by nitrate itself, negative control operates downstream of nitrate reduction/assimilation. As a result, there is a delay in the activation of the negative feedback compared to the positive one. Graphically, this behavior is reflected in the formation of a peak in net-uptake rate of nitrate.

Our model is mainly devised for lower concentrations of nitrate working in a range of nitrate (micromolar) when HATS mainly contributes to the absorption of the anion in plants. However, according to Muños et al. (2004) and Krouk et al. (2006), we have taken into account another level of regulation: a self-inhibition of the high-affinity nitrate acquisition that occurs when a high external concentration of nitrate is available in nutrient solution (see Figure S2 and Data S1). We can speculate that multilevel regulation is necessary to enable the system to control the acquisition of nitrate when it is not required, thereby preventing excess accumulation of the nutrient. Indeed, the model suggests that ammonium inhibition operates in the middle term, while the action of glutamine and other amino acids ensures a long-term effect by acting as a memory or, drawing a comparison to human digestion, a signal of satiety for the system. Thus, depending on the amino acid concentration (i.e., glutamine), the system can maintain a negative control on nitrate acquisition even in the long term when ammonium is fully assimilated.

Our model can be useful to predict and thus investigate the influence of the different components on the nitrate uptake dynamic. For example, when ammonium is present in the root external media, the experimental results indicated that the presence of ammonium modified the pattern of net-nitrate influx rate over time. In particular, increasing ammonium concentration in the root external solution causes an ever-lowering of the maximum achievable nitrate uptake rate (Figure 1). The model fits well with the experimental data (Figure 3), indicating that the influx of nitrate in root cell is regulated by ammonium concentration at cellular level (Figure 2). It is expected that the root exposure to ammonium in the root external solution determined an increase of ammonium concentration in the root cells, anticipating the occurrence of feedback inhibition on the nitrate acquisition system in comparison to no-ammonium treated plants

FIGURE 6 Comparison of the model simulation (blue lines) with the experimental data measured in different plant species: (A, B) *Vitis vinifera* (Sauvignon, dataset O; Chardonnay, dataset P; Tomasi et al., 2015); (C) *Triticum aestivum* (var. Palladio, dataset Q); (D) *Beta vulgaris* (var. Saccharifera, dataset R; Monte et al., 2006); (E) *Arabidopsis thaliana* (Columbia 0, dataset S; Massaro et al., 2019); (F, G) *Z. mays* (P0423, dataset T; PR33T56, dataset U; Zanin et al., 2015). Red asterisks refer to the range, above and below, of ±standard deviation from the average values collected by experimental analyses. The alphabetic numerals of the datasets refer to Table S1

(*Nitrate* plants; Glass et al., 2002). Indeed, the shape of the nitrate net uptake rate was characterized by a gradual reduction of maximum nitrate influx in root cells as a consequence of the ammonium concentration applied to the nutrient solution (Figures 1 and 3).

The storage of nitrate in the vacuole or the compartmentalization of transporters in vesicles, corresponding to variable x_6, has an important role in the process. We tried to simplify the model by removing the components of nitrate and transporter compartmentalization, but the output did not fit the experimental data well. This implies that these components are relevant in regulating the system, and we can speculate that their occurrence might ensure the resilience of plants to environmental changes by facilitating fast adaptation.

Actually, we tried to reduce the complexity in several ways. We adopted a model with three differential equations for the current variables x_1 and x_5, introducing a new aggregate variable x_a to take into account the negative part of the feedback. This simpler third-order model produces poor prediction results (data not shown). We also reduced model complexity by eliminating variables x_6 and x_7, by namely neglecting the vacuole role in the process by assuming $\dot{x_7} = \mu x_1 - \nu x_7 = 0$, $\dot{x_6} = \rho x_5 - \sigma x_6 = 0$, so reducing the system to five differential equations. This modest simplification slightly compromises the fitting results (data not shown).

As mentioned above, our model was validated also on plant species other than maize. The fitting of parametric values allowed us to generate a model that fitted with the experimental data. The validation of our model on some plant species demonstrated its relevance for the prediction of plant response to nitrate availability. A future possible exploitation of the model will include the prediction of the effect of biostimulants and of different N-forms on nitrate acquisition in plants, which presumably would alter some relevant parameters of the model, in particular u_1.

The use of a multidisciplinary approach has generated a model of nitrate absorption that aims to contribute to the rational use of N fertilizers in agriculture aimed at producing high-quality crops with low environmental impact. Moreover, within the context of precision agriculture, implementing the model in SEMoLa (*NitrUp* package) would be a valuable tool for farmers to predict the dynamics of nitrate acquisition in crops based on the anion concentration in the soil solution.

AUTHOR CONTRIBUTIONS

All authors contributed to the study conception, design, data collection, analyses, and manuscript preparation. All authors read and approved the final manuscript.

ACKNOWLEDGMENTS

This work was supported by the Departmental Strategic Plan (PSD) of the University of Udine-Interdepartmental Project on Artificial Intelligence (2020–25). This study was carried out within the Agritech National Research Center and received funding from the European Union Next-Generation EU (Piano Nazionale di Ripresa e Resilienza (PNRR)–Missione 4 Componente 2, Investimento 1.4–D.D. 1032 17/06/2022, CN00000022) and by the European Union Next-Generation EU (Grant Number Uniud-DM737). This manuscript reflects only the authors' views and opinions, neither the European Union nor the European Commission can be considered responsible for them.

DATA AVAILABILITY STATEMENT

The data that support the findings of this study are available in the Supporting Information of this article.

ORCID

Laura Zanin https://orcid.org/0000-0002-3840-9843

REFERENCES

Araki, R. & Hasegawa, H. (2006) Expression of rice (*Oryza sativa* L.) genes involved in high-affinity nitrate transport during the period of nitrate induction. *Breeding Science*, 56, 295–302.

Araya, T., Kubo, T., von Wirén, N. & Takahashi, H. (2016) Statistical modeling of nitrogen-dependent modulation of root system architecture in *Arabidopsis thaliana*. *Journal of Integrative Plant Biology*, 58, 254–265.

Aslam, M., Travis, R.L. & Huffaker, R.C. (1993) Comparative induction of nitrate and nitrite uptake and reduction systems by ambient nitrate and nitrite in intact roots of barley (*Hordeum vulgare* L.) seedlings. *Plant Physiology*, 102, 811–819.

Balconi, C., Brosio, D. & Motto, M. (1997) Analysis of nitrogen partitioning in maize. *Maize Genetics Cooperation Newsletter*, 71, 10–11.

Barberon, M., Dubeaux, G., Kolb, C., Isono, E., Zelazny, E. & Vert, G. (2014) Polarization of iron-regulated transporter 1 (IRT1) to the plant-soil interface plays crucial role in metal homeostasis. *Proceedings of the National Academy of Sciences of the United States of America*, 111, 8293–8298.

Behl, R., Tischner, R. & Raschke, K. (1988) Induction of a high-capacity nitrate-uptake mechanism in barley roots prompted by nitrate uptake through a constitutive low-capacity mechanism. *Planta*, 176, 235–240.

Boer, M.D., Santos Teixeira, J. & Ten Tusscher, K.H. (2020) Modeling of root nitrate responses suggests preferential foraging arises from the integration of demand, supply and local presence signals. *Frontiers in Plant Science*, 11, 708.

Cacco, G., Sidari, M., Gelsomino, A. & Orsega, E.F. (2002) An attempt to model the induction and feedback inhibition of nitrate uptake in wheat seedlings. *Journal of Plant Nutrition*, 25, 17–25.

Cárdenas-Navarro, R., Adamowicz, S., Gojon, A. & Robin, P. (1999) Modelling nitrate influx in young tomato (*Lycopersicon esculentum* Mill.) plants. *Journal of Experimental Botany*, 50, 625–635.

Cataldo, D.A., Haroon, M., Schrader, L.F. & Youngs, V.L. (1975) Rapid colorimetric determination of nitrate in plant tissue by nitration of salicylic acid. *Communications in Soil Science and Plant Analysis*, 6, 71–80.

Cesco, S., Chiani, A., Pinton, R. & Varanini, Z. (2002) Assorbimento di NO_3^- in radici di barbabietola da zucchero (*Beta vulgaris* L. var saccharifera): prima caratterizzazione. *Agroindustria*, 2, 146–150.

Daniel-Vedele, F., Filleur, S. & Caboche, M. (1998) Nitrate transport: a key step in nitrate assimilation. *Current Opinion in Plant Biology*, 1, 235–239.

Danuso, F. & Rocca, A. (2014) SEMoLa: a simple and easy modelling language. *Ecological Modelling*, 285, 54–77.

Devienne-Barret, F., Justes, E., Machet, J.M. & Mary, B. (2000) Integrated control of nitrate uptake by crop growth rate and soil nitrate availability under field conditions. *Annals of Botany*, 86, 995–1005.

Forrester, J. W. (1968) *Principles of Systems*. Cambridge, MA: Wright-Allen Press, Inc.

Garnett, T., Plett, D., Conn, V., Conn, S., Rabie, H., Rafalski, J.A. et al. (2015) Variation for N uptake system in maize: genotypic response to N supply. *Frontiers in Plant Science*, 6, 936.

Glass, A.D. (2003) Nitrogen use efficiency of crop plants: physiological constraints upon nitrogen absorption. *Critical Reviews in Plant Sciences*, 22, 453–470.

Glass, A.D., Britto, D.T., Kaiser, B.N., Kinghorn, J.R., Kronzucker, H.J., Kumar, A. et al. (2002) The regulation of nitrate and ammonium transport systems in plants. *Journal of Experimental Botany*, 53, 855–864.

Ho, C.H., Lin, S.H., Hu, H.C. & Tsay, Y.F. (2009) CHL1 functions as a nitrate sensor in plants. *Cell*, 138, 1184–1194.

Hole, D.J., Emran, A.M., Fares, Y. & Drew, M.C. (1990) Induction of nitrate transport in maize roots, and kinetics of influx, measured with nitrogen-13. *Plant Physiology*, 93, 642–647.

Ishiyama, K., Inoue, E., Tabuchi, M., Yamaya, T. & Takahashi, H. (2004) Biochemical background and compartmentalized functions of cytosolic glutamine synthetase for active ammonium assimilation in rice roots. *Plant & Cell Physiology*, 45, 1640–1647.

Jackson, W.A., Flesher, D. & Hageman, R.H. (1973) Nitrate uptake by dark-grown corn seedlings: some characteristics of apparent induction. *Plant Physiology*, 51, 120–127.

King, B.J., Siddiqi, M.Y. & Glass, A.D. (1992) Studies of the uptake of nitrate in barley: V. Estimation of root cytoplasmic nitrate concentration using nitrate reductase activity—implications for nitrate influx. *Plant Physiology*, 99, 1582–1589.

King, B.J., Siddiqi, M.Y., Ruth, T.J., Warner, R.L. & Glass, A.D. (1993) Feedback regulation of nitrate influx in barley roots by nitrate, nitrite, and ammonium. *Plant Physiology*, 102, 1279–1286.

Kotur, Z., Mackenzie, N., Ramesh, S., Tyerman, S.D., Kaiser, B.N. & Glass, A.D. (2012) Nitrate transport capacity of the Arabidopsis thaliana NRT2 family members and their interactions with AtNAR2.1. *New Phytologist*, 194, 724–731.

Kronzucker, H.J., Siddiqi, M.Y. & Glass, A.D. (1995) Kinetics of NO_3-influx in spruce. *Plant Physiology*, 109, 319–326.

Krouk, G., Lacombe, B., Bielach, A., Perrine-Walker, F., Malinska, K., Mounier, E. et al. (2010b) Nitrate-regulated auxin transport by NRT1.1 defines a mechanism for nutrient sensing in plants. *Developmental Cell*, 18, 927–937.

Krouk, G., Mirowski, P., LeCun, Y., Shasha, D.E. & Coruzzi, G.M. (2010a) Predictive network modeling of the high-resolution dynamic plant transcriptome in response to nitrate. *Genome Biology*, 11, 1–19.

Krouk, G., Tillard, P. & Gojon, A. (2006) Regulation of the high-affinity NO_3^- uptake system by NRT1.1-mediated NO_3-demand signaling in Arabidopsis. *Plant Physiology*, 142, 1075–1086.

Le Deunff, E. & Malagoli, P. (2014) An updated model for nitrate uptake modelling in plants. I. Functional component: cross-combination of flow–force interpretation of nitrate uptake isotherms, and environmental and in planta regulation of nitrate influx. *Annals of Botany*, 113, 991–1005.

Le Deunff, E., Malagoli, P. & Decau, M.L. (2019) Modelling nitrogen uptake in plants and phytoplankton: advantages of integrating flexibility into the spatial and temporal dynamics of nitrate absorption. *Agronomy*, 9, 116.

Lejay, L., Tillard, P., Lepetit, M., Olive, F., Filleur, S., Daniel-Vedele, F. et al. (1999) Molecular and functional regulation of two equation NO_3^- uptake systems by N- and C-status of Arabidopsis plants. *The Plant Journal*, 18, 509–519.

Li, W., Wang, Y., Okamoto, M., Crawford, N.M., Siddiqi, M.Y. & Glass, A.D. (2007) Dissection of the AtNRT2.1: AtNRT2.2 inducible high-affinity nitrate transporter gene cluster. *Plant Physiology*, 143, 425–433.

Liu, Q., Chen, X., Wu, K. & Fu, X. (2015) Nitrogen signaling and use efficiency in plants: what's new? *Current Opinion in Plant Biology*, 27, 192–198.

Locci, G., Santi, S., Monte, R., Pinton, R. & Varanini, Z. (2001) Involvement of plasma membrane H+-ATPase in nitrate uptake by maize genotypes. In: Horst, W.J., Schenk, M.K., Bürkert, A., Classsen, N., Flessa, H., Frommer, W.B. et al. (Eds.) *Plant nutrition-food security and sustainability of agro-ecosystems through basic and applied research*. Dordrecht: Springer, pp. 184–185.

Maghiaoui, A., Gojon, A. & Bach, L. (2020) NRT1.1-centered nitrate signaling in plants. *Journal of Experimental Botany*, 71, 6226–6237.

Malagoli, P., Lainé, P., Le Deunff, E., Rossato, L., Ney, B. & Ourry, A. (2004) Modeling nitrogen uptake in oilseed rape cv capitol during a growth cycle using influx kinetics of root nitrate transport systems and field experimental data. *Plant Physiology*, 134, 388–400.

Malagoli, P. & Le Deunff, E. (2014) An updated model for nitrate uptake modelling in plants. II. Assessment of active root involvement in nitrate uptake based on integrated root system age: measured versus modelled outputs. *Annals of Botany*, 113, 1007–1019.

Massaro, M., De Paoli, E., Tomasi, N., Morgante, M., Pinton, R. & Zanin, L. (2019) Transgenerational response to nitrogen deprivation in *Arabidopsis thaliana*. *International Journal of Molecular Sciences*, 20, 5587.

Miller, A.J., Fan, X., Orsel, M., Smith, S.J. & Wells, D.M. (2007) Nitrate transport and signalling. *Journal of Experimental Botany*, 58, 2297–2306.

Min, X., Siddiqi, M.Y., Guy, R.D., Glass, A.D.M. & Kronzucker, H.J. (1998) Induction of nitrate uptake and nitrate reductase activity in trembling aspen and lodgepole pine. *Plant, Cell & Environment*, 21, 1039–1046.

Monte, R., Cesco, S., Pinton, R. & Varanini, Z. (2006) Acquisizione di nitrato e ammonio in radici di barbabietola da zucchero (*Beta vulgaris* L var saccharifera): caratterizzazione cinetica ed effetti sull'accumulo di saccarosio. *Agroindustria*, 5, 177–184.

Muños, S., Cazettes, C., Fizames, C., Gaymard, F., Tillard, P., Lepetit, M. et al. (2004) Transcript profiling in the chl1-5 mutant of Arabidopsis reveals a role of the nitrate transporter NRT1.1 in the regulation of another nitrate transporter, NRT2.1. *Plant Cell*, 16(9), 2433–2447.

Nakano, S., Takahashi, M., Sakamoto, A., Morikawa, H. & Katayanagi, K. (2012) Structure–function relationship of assimilatory nitrite reductases from the leaf and root of tobacco based on high-resolution structures. *Protein Science*, 21, 383–395.

Nazoa, P., Vidmar, J.J., Tranbarger, T.J., Mouline, K., Damiani, I., Tillard, P. et al. (2003) Regulation of the nitrate transporter gene AtNRT2.1 in Arabidopsis thaliana: responses to nitrate, amino acids and developmental stage. *Plant Molecular Biology*, 52, 689–703.

Orsel, M., Chopin, F., Leleu, O., Smith, S.J., Krapp, A., Daniel-Vedele, F. et al. (2006) Characterization of a two-component high-affinity nitrate uptake system in Arabidopsis. Physiology and protein–protein interaction. *Plant Physiology*, 142, 1304–1317.

Orsel, M., Filleur, S., Fraisier, V. & Daniel-Vedele, F. (2002) Nitrate transport in plants: which gene and which control? *Journal of Experimental Botany*, 53, 825–833.

Pii, Y., Alessandrini, M., Guardini, K., Zamboni, A. & Varanini, Z. (2014) Induction of high-affinity NO_3^- uptake in grapevine roots is an active process correlated to the expression of specific members of the NRT2 and plasma membrane H^+-ATPase gene families. *Functional Plant Biology*, 41, 353–365.

Pinton, R., Cesco, S., Iacolettig, G., Astolfi, S. & Varanini, Z. (1999) Modulation of uptake by water-extractable humic substances: involvement of root plasma membrane H^+-ATPase. *Plant and Soil*, 215, 155–161.

Pinton, R., Tomasi, N. & Zanin, L. (2016) Molecular and physiological interactions of urea and nitrate uptake in plants. *Plant Signaling & Behavior*, 11, e1076603.

Santi, S., Locci, G., Monte, R., Pinton, R. & Varanini, Z. (2003) Induction of nitrate uptake in maize roots: expression of a putative high-affinity nitrate transporter and plasma membrane H^+-ATPase isoforms. *Journal of Experimental Botany*, 54, 1851–1864.

Segonzac, C., Boyer, J.C., Ipotesi, E., Szponarski, W., Tillard, P., Touraine, B. et al. (2007) Nitrate efflux at the root plasma membrane: identification of an Arabidopsis excretion transporter. *Plant Cell*, 19, 3760–3777.

Siddiqi, M.Y., Glass, A.D., Ruth, T.J. & Fernando, M. (1989) Studies of the regulation of nitrate influx by barley seedlings using $^{13}NO_3^-$. *Plant Physiology*, 90, 806–813.

Tan, S., Zhang, X., Zhang, Q., Li, Y.M., Zhang, P. & Yin, L.P. (2022) HRM and CRAC in MxIRT1 act as iron sensors to determine MxIRT1 vesicle-PM fusion and metal transport. *Plant Signaling & Behavior*, 17, 2005881.

Tomasi, N., Monte, R., Varanini, Z., Cesco, S. & Pinton, R. (2015) Induction of nitrate uptake in sauvignon blanc and chardonnay grapevines depends on the scion and is affected by the rootstock. *Australian Journal of Grape and Wine Research*, 21, 331–338.

Varanini, Z., Cesco, S., Tomasi, N., Pinton, R., Guzzo, F., Zamboni, A. et al. (2018) Nitrate induction and physiological responses of two maize lines differing in nitrogen use efficiency: effects on N availability, microbial diversity and enzyme activity in the rhizosphere. *Plant and Soil*, 422, 331–347.

Vidal, E.A., Alvarez, J.M., Araus, V., Riveras, E., Brooks, M.D., Krouk, G. et al. (2020) Nitrate in 2020: thirty years from transport to signaling networks. *Plant Cell*, 32, 2094–2119.

Wang, R., Liu, D. & Crawford, N.M. (1998) The Arabidopsis CHL1 protein plays a major role in high-affinity nitrate uptake. *Proceedings of the National Academy of Sciences of the United States of America*, 95, 15134–15139.

Wirth, J., Chopin, F., Santoni, V., Viennois, G., Tillard, P., Krapp, A. et al. (2007) Regulation of root nitrate uptake at the NRT2. 1 protein level in *Arabidopsis thaliana*. *Journal of Biological Chemistry*, 282, 23541–23552.

Zamboni, A., Astolfi, S., Zuchi, S., Pii, Y., Guardini, K., Tononi, P. et al. (2014) Nitrate induction triggers different transcriptional changes in a high and a low nitrogen use efficiency maize inbred line. *Journal of Integrative Plant Biology*, 56, 1080–1094.

Zanin, L., Nerva, L., Alessandrini, M., Tomasi, D., Pinton, R., Lucchetta, M. et al. (2022) Effects of the fractionation of the nitrogen fertilization on root nitrate uptake and vine agronomic performance in pinot Gris grapevines in a temperate climate. *Journal of Soil Science*, 22, 4996–5008.

Zanin, L., Tomasi, N., Zamboni, A., Sega, D., Varanini, Z. & Pinton, R. (2018) Water-extractable humic substances speed up transcriptional response of maize roots to nitrate. *Environmental and Experimental Botany*, 147, 167–178.

Zanin, L., Zamboni, A., Monte, R., Tomasi, N., Varanini, Z., Cesco, S. et al. (2015) Transcriptomic analysis highlights reciprocal interactions of urea and nitrate for nitrogen acquisition by maize roots. *Plant & Cell Physiology*, 56, 532–548.

Zhuo, D., Okamoto, M., Vidmar, J.J. & Glass, A.D. (1999) Regulation of a putative high-affinity nitrate transporter (Nrt2;1At) in roots of *Arabidopsis thaliana*. *Plant Journal*, 17, 563–568.

SUPPORTING INFORMATION

Additional supporting information can be found online in the Supporting Information section at the end of this article.

How to cite this article: Zanin, L., Tomasi, N., Casagrande, D., Danuso, F., Buoso, S., Zamboni, A. et al. (2023) A mechanistic mathematical model for describing and predicting the dynamics of high-affinity nitrate intake into roots of maize and other plant species. *Physiologia Plantarum*, 175(5), e14021. Available from: https://doi.org/10.1111/ppl.14021